JETIR.ORG ISSN: 2349-5162 | ESTD Year : 2014 | Monthly Issue

JOURNAL OF EMERGING TECHNOLOGIES AND INNOVATIVE RESEARCH (JETIR)

An International Scholarly Open Access, Peer-reviewed, Refereed Journal

THE TECHNICAL PAST AND PRESENT OF SALT SPRAY

Askari Imam Khan[1], Dr. Praveen Kumar[2]

[1]Research Scholar, Sardar Patel University, Balaghat (M.P)
[2]Research Supervisor, Sardar Patel University, Balaghat (M.P)

ABSTRACT

During salt spray accelerated corrosion testing, coated samples are subjected to a corrosive attack in order to evaluate (mostly quantitatively) the coating's suitability for use as a protective finish. To lessen the severity of this problem, the automotive industry has employed friction stir spot joining and mechanical fastening processes like the self-pierce riveting method. This paper presents the results of an experimental investigation into the mechanical properties of annealed and unannealed AA1100 sheet of 0.5mm thickness and a comparison of these two materials. Annealed and unannealed AA1100 are subjected to tensile, flexural, and drop impact tests to establish their mechanical properties. The corrosion resistance of annealed and unannealed AA1100 was evaluated using a salt spray test.

KEYWORDS: AA1100, Tensile Test, Flexural Test, Drop Impact Test, Salt Spray Test

INTRODUCTION

Standardized and widely used, the salt spray test (also known as the salt fog test) evaluates a material's or coating's ability to withstand corrosion in the field. Materials typically tested are metals (though stone, ceramics, and polymers may also be tested) with a protective coating applied to the surface to prevent corrosion.

Accelerated corrosion testing with salt spray creates a corrosive assault on coated samples to assess (mainly comparative) the coating's fitness for usage as a protective finish. After a certain amount of time has passed, the presence of corrosion byproducts (rust or other oxides) is assessed. The coating's ability to prevent corrosion or rust has a direct impact on how long tests can go without revealing the presence of corrosion or rust.

When it comes to corrosion testing, the salt spray test is among the most well-known and time-honored options. When it was first published in 1939, ASTM B117 became the first salt spray standard to be accepted worldwide. ISO 9227, JIS Z 2371, and ASTM G85 are a few further related international standards.

Use of lightweight materials like aluminum and magnesium alloys has been on the rise in the automotive industry for some time now. This is because of the industry's desire to reduce the overall weight of vehicle bodies. When aluminum alloys and steels are joined using a standard fusion welding process, the generation of FexAly brittle intermetallic compounds at the joining interface is inevitable, significantly weakening the resulting weld. A number of different mechanical fastening processes, including self-pierce riveting, have been tried in the automotive industry in an effort to reduce this issue. When compared to resistance spot welding, the low productivity and subsequent increase in manufacturing costs that result from using friction stir spot joining and mechanical fastening processes is a major drawback. Since production rates and

quantities for car bodies tend to be high, automated resistance spot welding is an excellent choice for the necessary welding process. As a result, the automotive industry makes extensive use of this method of welding. Resistance spot welding, used for joining dissimilar metals, can produce asymmetrical welds due to the materials' varying thermal conductivity, electrical resistivity, and melting point.

LITRATURE OF REVIEW

Sathish, T et.al (2021) The primary goals of this study are to improve the corrosion resistance and mechanical strength of a hybrid matrix made of an aluminum alloy. Stir casting is used to prepare the composites. The process starts with an aluminum alloy 8079 base material and adds reinforcing particles made of titanium nitride and zirconium dioxide. Fabricated AA8079/TiN + ZrO2 composites perform well in mechanical tests such ultimate tensile strength, wear, salt spray corrosion test, and microhardness test. The process parameters of the mechanical and corrosion tests are optimized using L9 OA statistical analysis. Analysis of variance (ANOVA) isolates the significance of each variable. The tensile and wear test conditions are set by selecting a percentage of reinforcement (3%, 6%, or 9%), a speed of churning (500, 550, or 600 rpm), and a duration of stirring (60, 90, or 120 seconds) (20, 25 and 30 min). Equally important in both the salt spray and microhardness tests is the choice of reinforcement percentage (3%, 6%, and 9%), pH value (3, 6, and 9), and hang duration (24, 48 and 72 h).

Zhi-ChaoHuang et.al (2022) Light weighting vehicles is a priority for the automotive industry's future growth, therefore it's only natural that these materials will eventually be fused together. In order to combine dissimilar materials, a novel technique known as self-piercing riveting (SPR) has been developed. Sheets of AA6061 and DP590 were developed for SPR and SPR-bonded (SPR-A) joints. After exposing SPR and SPR-A joints to neutral salt spray conditions for varying amounts of time, their mechanical characteristics were evaluated. With more time in the salt spray, the joints' shear and fatigue qualities degraded. When comparing SPR and SPR-A joints subjected to the same amount of salt spray time, the latter exhibit lower maximum failure loads whereas the former exhibit greater energy absorption values during shear testing. Results from fatigue tests indicated that fretting wear between the rivet-foot and the bottom sheet is the primary failure mechanism of joints. Furthermore, there is no discernible relationship between the fatigue failure modes of the two types of joints and the amount of time exposed to salt spray.

Salman Farishi et.al (2021) This paper presents the results of an experiment to evaluate the durability of a commercially available glass fibre reinforced polyester composite by subjecting it to accelerated salt spray (fog). The effects of salt spray on the ageing of materials were investigated by measuring their mechanical characteristics, specifically their flexural stress and flexural modulus. The Copper-Accelerated Acetic Acid Salt Spray (CASS) Test under ASTM B368 was used to simulate prolonged exposure to salt spray. The CASS experiment lasted 120 hours with 24-hourly checks. The results of a flexural modulus test tend to remain stable for up to four days, but undergo a more noticeable shift on the fifth day of testing. In addition, Scanning Electron Microscopy (SEM) findings on the morphology of specimens (SEM). In addition, the SEM analysis revealed no damage other than superficial scratching to the tested specimens.

Huai Chen et.al (2019) The optical features of the sun selective absorber coating (SSAC) have a significant role in the collector's thermal performance, making it an essential part of every solar collector. The solar absorptance (radiation absorbed by the material) and thermal emittance (radiation emitted by the material) are the most important measures of an SSAC's optical characteristics (emittance for long-wave radiation). Some high-performing SSACs, however, have drawbacks like decreased durability and resistance to corrosion and abrasion, which is especially harmful for SSACs because, for example, chlorides in the atmosphere have become a main contributor to corrosion in coastal areas with the increasing trend of global warming. In order to compare the impact of salt spray testing on the optical properties of SSACs made with different manufacturing techniques, this paper subjects SSACs made with three common techniques to the test for 12 hours, 24 hours, 36 hours, and 48 hours. These techniques are anode oxidation (AO), vacuum magnetron sputtering (VMS), and black chromium plating (BCP).

J.R. Jessy Michla et.al (2022) This study employs the neutral salt spray (NSS) technique to examine the effects of nitriding temperatures of 530, 560, and 580 °C for 2 hours on the corrosion resistance of additively manufactured (AM) 17-4 PH steels over 104 hours. Columnar grains were found in the built direction of the additive manufacturing process, according to the morphological analysis. Increases in nitriding temperature led to larger refined grains and more precipitates. An analysis revealed that at 580

degrees Celsius, a passive oxide layer and nitrogen-rich precipitates formed on the surface, resulting in the least amount of weight loss. The nitrided sample failed the salt spray test, as evidenced by the presence of Cr2N, (Fe, Cr)4N, (Fe, Cr)2-3N, Fe2O3, FeOOH, and Cr2O3 as determined by X-ray diffraction (XRD).

METHODOLOGY

Tensile, flexural, salt spray, and drop impact test specimens were collected in both their unannealed and annealed states. In order to determine the qualities of a material, three samples are obtained in each direction of the tensile test (i.e., 00, 450, 900), using AA110.

EXPERIMENTAL PROCEDURE

Both annealed and unannealed variations of the AA1100 aluminum alloys were studied. The experimental details are described in the following. Specimens were sliced from a 0.5mm thick sheet in three directions, parallel (00), perpendicular (450), and perpendicular (900) to the rolling axes of the aluminum sheet metal.

Tensile Test

In order to conduct the tensile tests, a 12.5 mm wide by 50 mm long test specimen was used in accordance with ASTM B557. The tensile test, both annealed and non-annealed, is the most common test for sheet metal's formability. The material tested in the current investigation is shown in Fig. 1.

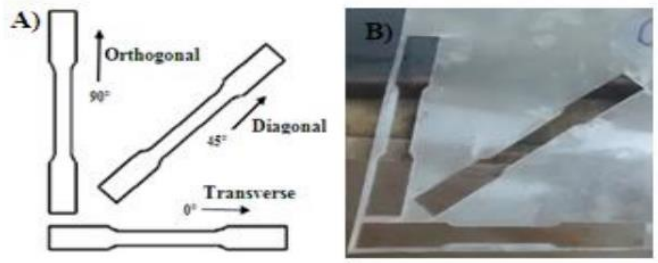

Figure 1 A. Specimen Orientation of rolling direction

Preparation of Tensile Test Specimen

According to Fig. 1, the tensile test specimens were oriented at 0, 45, and 90 degrees with respect to the rolling directions of the sheet metal blank. The specimens were annealed at 440°C temperature with soaking period of 4 Hours 15 min and then cooled in furnace itself. Materials with a better grain structure, thanks to soaking [17]. The sample is then cooled down in a furnace. Extensometer was used to record the lengths of all experiments conducted at room temperature. The sheet is rolled in three different orientations for this experiment: parallel (0), diagonally, and perpendicularly. In order to measure mechanical properties in tensile specimens were prepared with different specimen angles, 0° straight ply, 45° cross ply, and 90° normal ply, to the sheet rolling direction. In order to execute the tensile test, a servo-controlled Universal Testing Machine (UTM) was used. The specimen was put through a constant extensometer test. According to Fig. 2, tensile tests were conducted on samples using the FIE-UTM. Using a 400 KN UTM, the specimens were clamped at both ends and pulled at a consistent pace.

Figure 2 Tensile Specimen Setup in Universal Testing Machine

Flexural Test

The sheets were put through a flex test according to ASTM D790. The load was applied at the Center points of the span for the sandwich specimen that measured 150 mm in length, 30 mm in width, and 0.5 mm in thickness (Fig. 3).

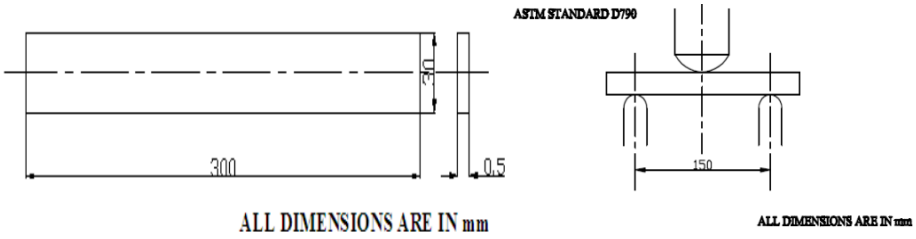

Figure 3 Flexural test specimen as per ASTM standard D790

The flexural test measures the modulus of elasticity, stress, and strain under bending conditions. Figure 2 shows a schematic of the test specimen used in the ASTM: D790 flexural test, which is performed using a three-point loading setup. The sample is placed between two supports and loaded at a consistent pace until it breaks. The term "flexural strength" refers to the highest stress in the fibre at the fiber's outermost end. The tensile tests on the sheet specimens are conducted using FIE-UTM, and the applied load and resulting displacements are documented. These tests are known as three-point sand and four-point bending, respectively, and the force is applied vertically at one or two locations. Stresses along the length of the specimens are tensile near the bottom and compressive near the top. This strain is determined using simple beam equations provided in the literature. A bending fracture's stress may be calculated using the transverse rupture strength. If a bending moment similar to that in Figure 4 were applied to the larger volume of the specimen, the likelihood of the presence of defects in this volume would increase. Thus, the modulus of rupture obtained from the four-point test is less than that obtained from the three-point test.

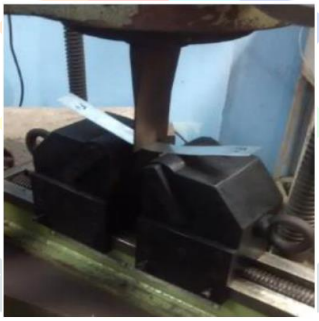

Figure 4 Flexural Specimen Setup in Universal Testing Machine

Drop Impact Test

The Charpy test, the Izod test, the drop weight impact test, the chip impact test, the Compression-After-Impact (CAI) test, and the Tension-After-Impact (TAI) test are the gold standards for determining the impact strength of metals. Considering the difficulties inherent in conducting impact testing on sheet metal, the drop weight impact test has replaced the more common Charpy and Izod tests. The Formability Analysis, Mechanical, and Corrosion Behavior of AA1100 Sheet Metal: Another Experimental Investigation IJMET 904 Editor@iaeme.com http://iaeme.com/Home/journal/IJMET The primary benefit of employing a drop weight impact test is that it simulates the circumstances to which the component would be exposed in actual use. There is no need to clamp the sample tightly while doing a drop weight impact test, unlike pendulum impact testing. The tup, an impact striker used in the drop weight impact technique, descends vertically via a guide tube to hit the centre of the specimen. Per ASTM standards, the guide tube's orientation relative to the impact surface must be perpendicular.

Salt Spray Corrosion Test

In Figure 5 we see a common corrosion test, the salt spray corrosion test, which is used to evaluate a material's resistance to corrosion. The majority of test items are metallic in nature and have a protective

coating applied to the surface to prevent corrosion. It is common knowledge that prolonged exposure to salt spray during an accelerated corrosion test will eventually lead to the formation of corrosion products/rust. One of the most common and well-known corrosion tests is the salt spray test. Use destructive testing methods on the coated samples to determine if the coating is up to the task of protecting the final product. After observing the specimen for a set amount of time, the degree of corrosion was assessed. How long a coating can withstand corrosion tests is a good indicator of how well it will perform in the field.

Figure 5 Salt Spray Corrosion Equipment

Microstructure Characterization

"Characterization" in the context of materials science is a catch-all term for any investigation into and measurement of a material's structure and characteristics. Its meaning can vary depending on who you ask; some restrict it to the study of microscopic structure techniques of materials, while others use it to refer to any materials analysis process that seeks to integrate the many macroscopic techniques available, such as mechanical testing, thermal analysis, and density calculation. Scales from atoms and chemical bonds to centimeters are all detected during the characterization of materials. This is especially true when examining coarse grain patterns in metals by imaging.

As a result of the topographical values and compositional information that their high-resolution, three-dimensional images provide, SEMs have found widespread use in a wide range of scientific and industrial contexts.

DATA ANALYSIS

Using the aforementioned methods, we measured the tensile and flexural properties, as well as the Salt Spray and Drop Impact resistance, of AA1100 aluminum alloy sheet metal specimens. For further discussion, the data was tabulated.

Tensile Properties

The mechanical behavior of the aluminum sheet is evaluated by means of tensile tests. Tensile specimens of 0.5 mm thick by 12.5 mm long aluminum sheet were created. The ultimate tensile strength (UTS) of a specimen is defined as the stress at which the cross section of the specimen begins to significantly contract during tensile testing.

Table 1 Tensile Properties of AA1100 Annealed Condition

Orientation relative to rolling direction	Annealed AA1100			
	n	k (MPa)	σ_y (MPa)	σ_u (MPa)
0°	0.1	8.6	61	665
45°	0.6	8.09	60	560
90°	0.13	8.1	63	540
Average	0.276	8.23	61.3	588.3

Standardization allows for accurate stress-strain curve prediction in Aluminum alloy AA 1100 sheet. Engineering strain-nominal stress curves for annealed and non-annealed sheets as determined by tensile tests are depicted in Figures 7 and 8, respectively. Analysis of the Formability, Mechanical, and Corrosion Behavior of AA1100 Sheet Metal Through Experiment

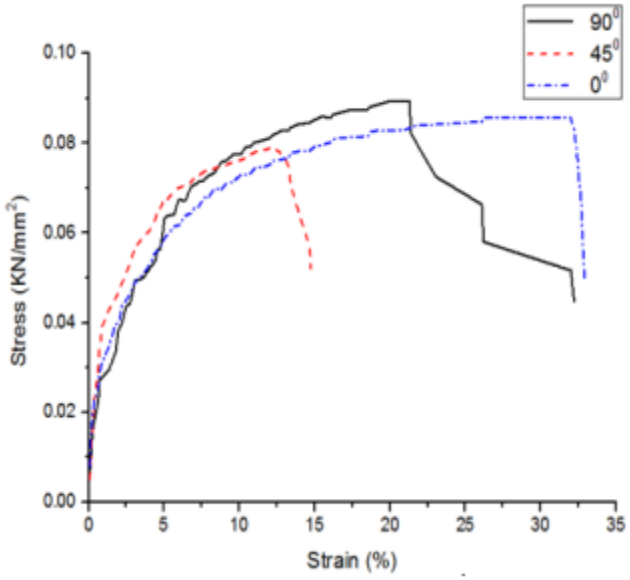

Figure 7 Stress-Strain Curves of Annealed AA1100

Table 2 Tensile Properties of AA1100 Un-Annealed Condition

Orientation relative to rolling direction	Un-Annealed AA1100			
	n	k (MPa)	σ_y (MPa)	σ_u(MPa)
0°	0.05	277	107.7	239.9
45°	0.1	13	38.6	137
90°	0.11	11.8	10.3	150
Average	0.086	100.6	52.2	175.6

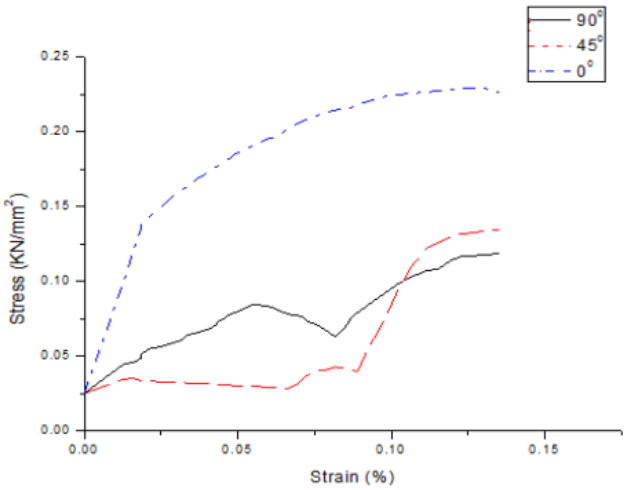

Figure 8 Stress-Strain Curves of Un-Annealed AA1100

Up to a well-defined yield point, it has shown a very linear stress–strain relationship. Determine the modulus of elasticity of a sample by locating the elastic region's linear part of the curve and taking its slope. In order to attain its Ultimate Tensile Strength, the tension must be raised by strain hardening. Poisson contractions up to this point have consistently shrunk the size of the cross section. Visual and real points of rupture are on the same vertical axis. For a given volume percent of reinforcement, a higher work hardening

rate may be achieved by increasing the volume fraction of reinforcement (and decreasing matrix volume). Early void development in the specimen is likely responsible for its reduced ductility.

Flexural Properties

In order to ascertain the flexural flexural strength of the aluminium skin material, flexural tests are typically performed. In comparison to tensile testing, the cost of a flexural test is much lower. The aluminium skin is laid flat over two contact points, and a force is applied to the top of the skin material from either contact point until the sample breaks. The flexural stress of a given sample is equal to the maximum force measured for that specimen.

Table 3 Flexural Strength of Annealed and Un-Annealed AA1100 Materials

Specimen	P(N)	D(mm)	S_f(N/mm)	σ_f(N/mm^2)
Annealed AA1100	30	13	2.3	625
Un Annealed AA 1100	60	14	4.08	703

It's difficult to get aluminum sheets to the right dimensions through shaping and machining. In addition, these samples are representative of surface flaws, and it can be a challenge to clamp brittle look-and-see samples for testing. Uneven stress distribution on the cross section may also result from a misaligned test specimen. The bend or flexure test, which typically employs a specimen with a rectangular cross section and is supported, is a rarely used testing method for brittle materials.

Drop Impact test (Annealed and Un-Annealed sheet)

No cracks were seen at a height of 2 kg weight fall from 100cm in either the annealed or un annealed AA 1100 material.

Salt Spray test

The table shows that the corrosion results of aluminum alloy with “NaCl” after salt spray corrosion for 24 h, the relatively wide in the activated states and these regions falls under the self-corrosion action to the potentials of the specimen, then arrived at the self-Corrosion potentials. This demonstrates a rise in resistance to corrosion.

MICROSTRUCTURE OF AA1100 SHEET METAL

Scanning Electron Microscopy (SEM) of an annealed specimen of AA1100 sheet material has revealed its grain structure. Microscopical analysis of unannealed AA1100 (Fig. 9) uncovered crystal structures of skin matrix with twinned grains, as well as step structures.

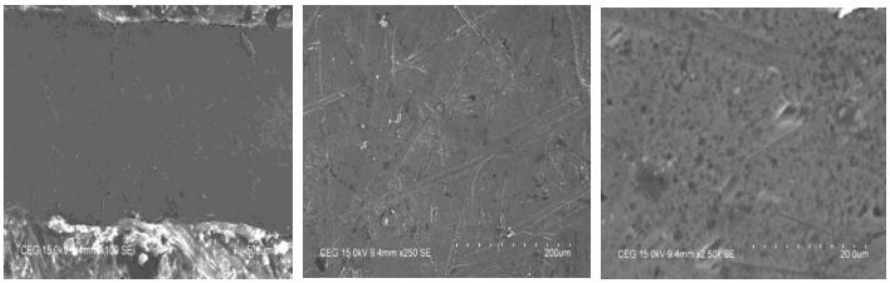

Figure 9 Represents Microstructure analysis using Scanning

Electron Microscopy (SEM) – Annealed sample of AA1100

Table 4 Observed test results of salt spray corrosion test

Initial Density gm/Cm^3	Area cm^2	Sample	Initial weight gm	Final weight gm	Weight loss Gm	Corrosion mm/Year	Corrosion mils/ Year
2.71	84.646	AA1100	10.836	10.834	0.002	1.5894E-05	0.00750175

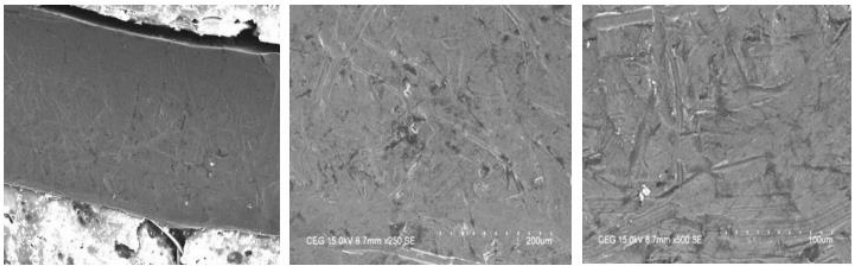

Fig.10. Represents SEM image of Un-Annealed sample AA1100-H14, (b), (c), Shows the magnified SEM images from various regions of (a) that helps us study the flaws due to which failure has occurred during macro characterization

CONCLUSION

The coating's ability to prevent corrosion or rust will determine how long a test can go on for; generally, the more corrosion-resistant a coating is, the longer it will take for rust or corrosion to appear. Low productivity and the resulting increase in manufacturing costs are one of the drawbacks of using friction stir spot joining and mechanical fastening processes instead of resistance spot welding. The results of the flexural tests show that material 00 performs the best. This demonstrates that this material can take in as much force as is applied to it without breaking, and that it can also distribute that force uniformly. The identical experimental test results for the Izod impact test indicate that both 00 and 900 have a good impact load. Because of this, they can withstand significant shock loads without breaking. The results obtained in both the salt spray and drop impact tests were simply superior in comparison to those of any monolithic sheet metal.

REFERENCES

1. Sathish, t.; mohanavel, v.; arunkumar, t.; raja, t.; rashedi, a.; alarifi, i.m.; badruddin, i.a.; algahtani, a.; afzal, a. Investigation of mechanical properties and salt spray corrosion test parameters optimization for aa8079 with reinforcement of tin + zro_2. *Materials* **2021**, *14*, 5260. Https://doi.org/10.3390/ma14185260

2. Zhi-chao huang, ying-lian jia, yu-qiang jiang, yong-chao zhang, mechanical properties and fatigue failure mechanisms of purely self-piercing riveted (spr) and hybrid (spr-bonded) joints under salt spray environment, journal of materials research and technology, volume 20, 2022, pages 2501-2517, issn 2238-7854,

3. Farishi, salman & wulandari, retno & rifathin, annisa & rusmana, dasep. (2021). The effect of accelerated salt spray exposure on mechanical properties of glass fiber reinforced polyester composite. Materials science forum. 1028. 223-227. 10.4028/www.scientific.net/msf.1028.223.

4. Huai chen wenfeng gao tao liu wenxian lin and ming li (2019) an experimental study on the efect of salt spray testing on the optical properties of solar selective absorber coatings produced with diferent manufacturing technologies

5. J.r. Jessy michla, nagarajan rajini, sikiru oluwarotimi ismail, t. Ram prabhu, faruq mohammad, suchart siengchin, m.p. Indira devi, effects of nitriding on salt spray corrosion resistance of additively manufactured 17-4 ph steels, materials letters, volume 330, 2023, 133258, issn 0167-577x,

6. Calabrese l, proverbio e, di bella g, galtieri g, borsellino c. Failure behaviour of spr joints after salt spray test. Eng structs 2015; 82:33e43. Https://doi.org/10.1016/ j. engstruct.2014.10.020.

7. Schanz j, nester s, meinhard d, pott t, riegel h, de silva anjali km, et al. Adhesively bonded cfrp/al joints: influence of the surface pretreatment on corrosion during salt spray test. Mater corros 2022;73(2):158e70. Https://doi.org/10.1002/ maco.202112752.

8. Calabrese l, galtieri g, borsellino c, di bella g, proverbio e. Durability of hybrid clinch-bonded steel/aluminum joints in salt spray environment. Int j adv manuf technol 2016; 87:3137e47. Https://doi.org/10.1007/s00170-016-8701-6.

9. Hao j, cong yj, zhang x, li gy, cui jj. Fatigue degradation after salt spray ageing of electromagnetically riveted joints for cfrp/al hybrid structure. Mater des 2018; 142:297e307. Https://doi.org/10.1016/j.matdes.2018.01.047.

10. Abe y, mori k. Mechanical clinching and self-pierce riveting for sheet combination of 780-mpa high-strength steel and aluminium alloy a5052 sheets and durability on salt spray test of joints. Int j adv manuf technol 2021; 113:59e72.

11. Kmec, j.; fechova, e.; hrehova, s. Optimization of parameters of the plastic-coated sheets at the corrosion test in salt spray. Mmsci. J. 2018,2018, 2167–2171.

12. Yao, k., song, k., wang, g., liang, m., xia, z., fan, j.: a discussion on the resistance performance to salt spray of solar selective absorber coatings. Chin. Sol. Energy 2013(7), 20–22 (2013)

13. Yin, z., zhou, x., wei, b.: evaluating the resistance performance to salt spray of solar selective absorber coatings. Chin. Sol. Energy 2013(9), 12–15 (2013)

14. Zhao h, han l, liu yp, liu xp. Analysis of joint formationmechanisms for self-piercing riveting (spr) process with varying joining parameters. J manuf process 2022;73:668e85. Https://doi.org/10.1016/j.jmapro.2021.11.038.

15. Achira s, abe y, mori k. Self-pierce riveting of three thin sheets of aluminum alloy a5052 and 980 mpa steel. Materials 2022;15. Https://doi.org/10.3390/ma15031010. 1010-1010.